Supporting Information

Wang et al. 10.1073/pnas.1006645107

SI Discussion

In birds, both the medial and lateral portions of the CM are auditory telencephalic nuclei and connected with the Field L via monosynaptic and/or polysynaptic pathways. In chicks, the boundaries between the medial and lateral CM are ambiguous. Although our injections were located mostly in the more medial portion of the CM, we chose to describe the studied mesopallium region using the more general nomenclature "caudal mesopallium" for accuracy.

The traditional definition of the Field L2 in birds contains two divisions, a medial portion (L2a) and a more laterally located portion (L2b). The present study focuses on the similarities between the avian L2a and the mammalian A1, both of which are primary cortical targets of the tonotopically organized lemniscal auditory system. In contrast, neurons in L2b receive auditory inputs from separate ascending pathways and exhibit broad frequency tuning. The equivalent component of the avian L2b in mammals remains unknown. The organization and connection of L2b were not examined in the present study.

It is noteworthy that the general pattern of intrinsic connections of the Field L/CM complex in chicks is consistent with that reported in previous studies in two other avian species. In zebra finches, each subunit of the complex (CM, L1, L2a, L3) connects with another subunit through reciprocal connections (1). We identified the majority of these connections in chicks, but found no evidence of a substantial projection of L1 to other regions of the Field L. In chicks, L1 provides a major output layer of the complex, consistent with studies in pigeons (2). The pattern of the intrinsic connectivity of the complex appears to be less complicated in pigeons than in zebra finches and chicks, with only two projections identified (2). These discrepancies across studies might be due to interspecies variation and/or technical limitations. Given the complexity of the interconnections across layers, exploration of the intrinsic detailed organization of the complex must be conducted at the individual cell level.

The remarkable similarities between the mammalian A1 neocortex and the avian auditory cortex, as described above, emphasize the need to reevaluate our concepts of the uniqueness of cortical networks in mammals and their evolutionary origins. These findings further challenge the views that the avian Field L/CM complex is homologous to a part of the mammalian amygdala, endopiriform area, or claustrum instead of A1 (3–7). This reasoning is based on selective data from gene expression and development, as well as a disputed direct thalamic input to the amygdala and claustrum, which has been interpreted as being homologous to the avian Ov-Field L pathway. However, the thalamic inputs to the claustrum and amygdala originate from the medial and dorsal divisions of the medial geniculate nucleus, the posterior intralaminar nucleus, and the suprageniculate nucleus (8), which are components of the secondary or nonlemniscal auditory pathway characterized by polysensory inputs in addition to broad frequency tuning and lack of tonotopy (9). In contrast, the avian Field L/CM and the mammalian A1 are the major telencephalic targets of the lemniscal auditory pathway via the mammalian MGv and the avian Ov, which are characterized by sharp frequency tuning and tonotopic organization (9). The distinctly different sensory inputs of the mammalian amygdala/claustrum and the avian Field L/CM provide strong evidence against the proposed homology of these two structures. Another important difference between these two structures is that amygdala and claustrum do not display a columnar internal organization, although they do contain complex intrinsic connections among its subdivisions (10, 11).

SI Materials and Methods

All experimental procedures used in this study were approved by the University of California San Diego's Animal Care and Use Committee and were in accordance with International Committee of Medical Journal Editors policy. Experiments were performed on White Leghorn chicks (*Gallus gallus*) of age <5 d.

In Vitro BDA Tracing and Intracellular Filling in Slice Preparations. The procedure has been described previously (12). Forty-one chicks were anesthetized with a mixture of 40 mg/kg of ketamine and 12 mg/kg of xylazine, and then decapitated. Brain slices (300 μm thick) through the Field L/CM complex were prepared in a modified coronal plane that may best conform to the radial plane or orientation first suggested by Bonke et al. (13). Layers of the complex were readily identified in wet tissue as four approximately parallel bands of differing brightness. BDA was injected extracellularly into individual layers using a glass electrode filled with 10% BDA either by pressure (30–150 nL in volume) or iontophoretically (positive current of 2–10 μA for 10 min). Intracellular filling of individual neurons was conducted in different slices with an electrode (100–300 MΩ) filled with 4% biocytin in 0.3 M KAc. Cell penetration was indicated by a sudden negative voltage drop and cell discharges. Biocytin was iontophoresed into the neuron with 2–3 nA of positive current for 3 min. Only one cell was filled in a single slice. Localization of BDA and biocytin were subsequently visualized by the standard avidin-biotin-peroxidase method, and sections were counterstained with Giemsa for identification of layers. In total, 21 slices with identifiable lamination, a clean BDA injection site, and good transportation of the tracer were chosen from 65 injected slices for data analyses; the injection sites are listed in Table S1. Nine neurons were filled intracellularly with their somata located in CM (n = 3), L1 (n = 1), L2 (n = 4), and L3 (n = 1).

Parvalbumin Immunocytochemistry. The procedure has been described previously (12). In brief, two chicks were transcardially perfused with 0.9% saline followed by 4% paraformaldehyde. After postfixation and sucrose equilibration of the brain, 30-μm coronal sections were acquired using a freezing sliding microtome. Free-floating sections were incubated with primary antibody solution (1:10,000; Sigma-Aldrich; lot #017H4821) overnight at 4 °C, followed by biotinylated anti-IgG antibody (1:200) for 1 h at room temperature. Localization of parvalbumin immunoreactivity was subsequently visualized by the standard avidin-biotin-peroxidase method. The localization pattern in the Field L/CM complex was consistent in the two chicks.

Cell Reconstruction and Measurement. Tracing of labeled neuronal structures after BDA extracellular injections was done with a camera lucida on a Zeiss WL microscope from individual resectioned 80-μm-thick sections. Slices with injections of BDA-conjugated rhodamine were observed and reconstructed using an Olympus FV-300 confocal microscope. For intracellularly filled neurons, axons from three adjacent 80-μm-thick sections containing the soma were reconstructed to provide a more complete tracing of axonal collaterals. The cell reconstructions were performed before Giemsa counterstaining to avoid obscuring fine cellular processes. All of the measurements, including soma size and dimensions of tracer transports, were done on calibrated images captured with a black and white (B/W) CCD camera, using Image software (National Institutes of Health). No corrections were made for tissue shrinkage.

1. Vates GE, Broome BM, Mello CV, Nottebohm F (1996) Auditory pathways of caudal telencephalon and their relation to the song system of adult male zebra finches. *J Comp Neurol* 366:613–642.
2. Wild JM, Karten HJ, Frost BJ (1993) Connections of the auditory forebrain in the pigeon (*Columba livia*). *J Comp Neurol* 337:32–62.
3. Bruce LL, Neary TJ (1995) The limbic system of tetrapods: A comparative analysis of cortical and amygdalar populations. *Brain Behav Evol* 46:224–234.
4. Striedter GF (1997) The telencephalon of tetrapods in evolution. *Brain Behav Evol* 49: 179–213.
5. Puelles L (2001) Thoughts on the development, structure and evolution of the mammalian and avian telencephalic pallium. *Philos Trans R Soc Lond B Biol Sci* 356:1583–1598.
6. Aboitiz F, Morales D, Montiel J (2003) The evolutionary origin of the mammalian isocortex: Towards an integrated developmental and functional approach. *Behav Brain Sci* 26:535–552.
7. Wullimann MF, Mueller T (2004) Teleostean and mammalian forebrains contrasted: Evidence from genes to behavior. *J Comp Neurol* 475:143–162.
8. Doron NN, Ledoux JE (1999) Organization of projections to the lateral amygdala from auditory and visual areas of the thalamus in the rat. *J Comp Neurol* 412:383–409.
9. Hu B (2003) Functional organization of lemniscal and nonlemniscal auditory thalamus. *Exp Brain Res* 153:543–549.
10. Pitkänen A, Amaral DG (1998) Organization of the intrinsic connections of the monkey amygdaloid complex: Projections originating in the lateral nucleus. *J Comp Neurol* 398:431–458.
11. Cassell MD, Freedman LJ, Shi C (1999) The intrinsic organization of the central extended amygdala. *Ann N Y Acad Sci* 877:217–241.
12. Wang Y, Luksch H, Brecha NC, Karten HJ (2006) Columnar projections from the cholinergic nucleus isthmi to the optic tectum in chicks (*Gallus gallus*): A possible substrate for synchronizing tectal channels. *J Comp Neurol* 494:7–35.
13. Bonke D, Scheich H, Langner G (1979) Responsiveness of units in the auditory neostriatum of the guinea fowl (*numida meleagris*) to species-species calls and synthetic stimuli, I: Tonotopy and functional zones of field L. *J Comp Physiol A* 132: 243–255.

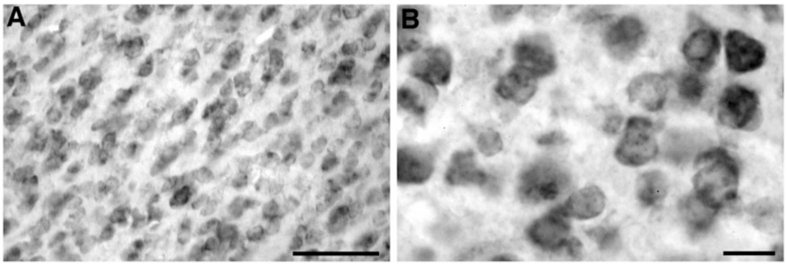

Fig. S1. Cytoarchitecture of Field L2a at low (*A*) and high (*B*) magnifications. Photos were taken from Nissl-stained sections and oriented the same way as in Fig. 1*D*, with dorsal at the top and medial to the right. The LaM was located dorsomedially to Field L2a. Note that granule cells in L2a tend to align in vertical stacks perpendicular to the layers. (Scale bar: 50 μm in *A*, 10 μm in *B*.)

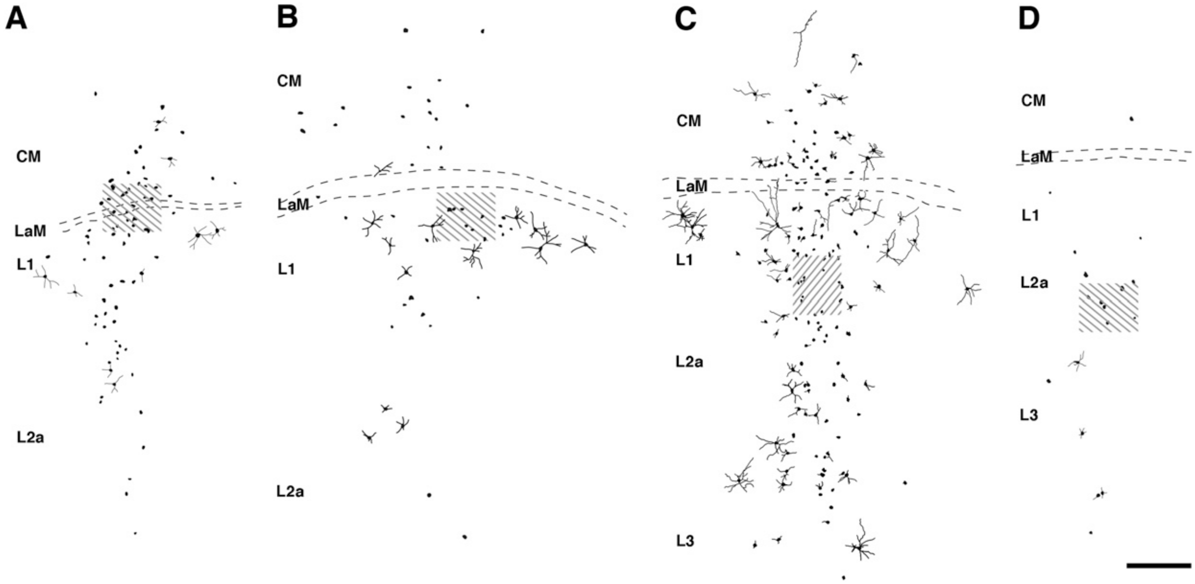

Fig. S2. Camera lucida reconstruction of labeled neurons after injection of BDA into CM/L1 (*A*), L1 (*B*), L1/L2a (*C*), and L2a/L3 (*D*). For clarity, labeled fibers are not shown. Note that the labeled neurons are located within a column crossing layers, regardless of the location and number of layers of deposition of the tracer. Shaded areas indicate the center of an injection site. Dashed lines outline the location of the LaM. (Scale bar: 200 μm.)

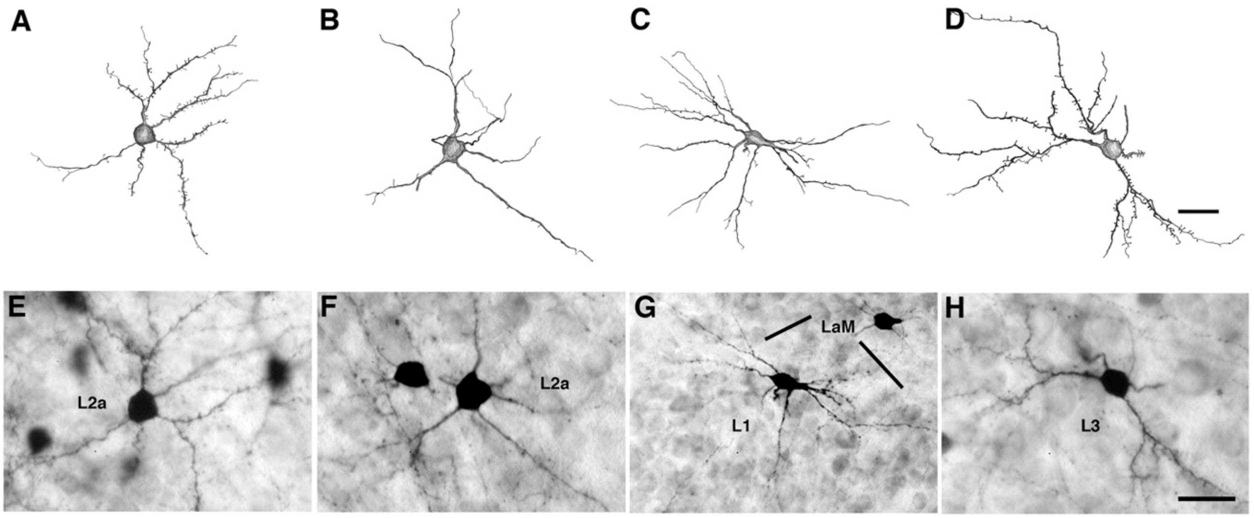

Fig. S3. Nongranule cell types in the Field L/CM complex revealed by BDA tracing studies. *A–D* show camera lucida reconstructions of the neurons illustrated in *E–H*, respectively. The neurons in *A* and *D* are spiny neurons, whereas those in *B* and *C* are relatively nonspiny. [Scale bars: 20 μm in *D* (applies to *A–D*), 20 μm in *H* (applies to *E–H*).]

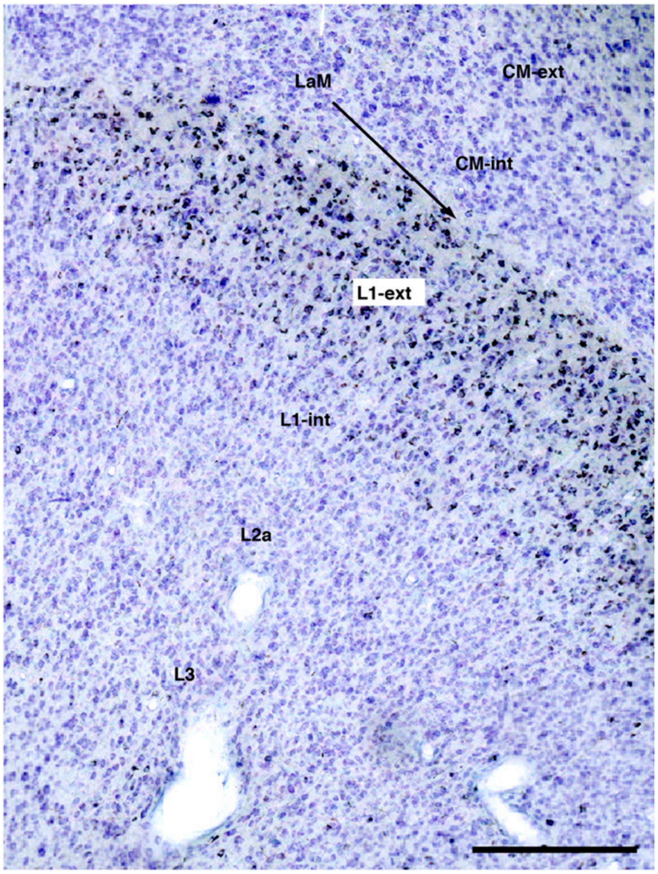

Fig. S4. Origin of the projection from the Field L/CM complex on Aivm. After an in vivo injection of CTB into the arcopallium, retrogradely labeled neurons within the Field L/CM complex were retricted to L1. Methods have been described in detail previously (4). The majority of the labeled neurons were found in L1 externus, with a very low density of labeled neurons detected in the internal portion of L1. There were no labeled neurons in CM, L2a, or L3, suggesting that L1 externus is a major output pathway of the Field/CM complex. The photo was taken from a Giemsa-counterstained section. Only CTB-containing cells were stained in black, with the remaining cells stained in blue. (Scale bar: 300 μm.)

Table S1. Injection site, injection method applied, and the distribution and number of labeled neurons following extracellular injections of BDA into the Field L/CM complex

Injection site	Injection method	Size of column (μm)*			Number of labeled neurons†			
		Long axis	Short axis	Ratio (%)	CM	L1	L2a	L3
CM	Pressure	1,251	573	46	—	11	12	4
CM	Pressure	1,135	635	56	—	11	28	0
CM	Pressure	1,291	587	45	—	17	9	1
CM	Iontophoresis	492	193	39	—	3	0	1
CM and L1-ext	Pressure	1,253	421	34	—	—	35	5
L1	Pressure	916	319	35	13	—	22	2
L1	Pressure	1,495	705	47	24	—	9	4
L1	Pressure	983	407	41	19	—	22	0
L1	Iontophoresis	1,405	465	33	22	—	6	4
L1-int and L2a	Pressure	1,705	894	52	49	—	—	10
L1-int and L2a	Iontophoresis	1,187	568	48	4	—	—	3
L1-int and L2a	Iontophoresis	1,748	765	44	14	—	—	5
L1 and L2a	Pressure	1,373	660	48	9	—	—	1
L1 and L2a	Iontophoresis	1,868	801	43	22	—	—	2
L2a	Pressure	1,653	341	21	16	1	—	10
L2a	Pressure	1,355	667	49	12	6	—	10
L2a	Pressure	1,359	631	46	4	1	—	5
L2a	Pressure	1,288	323	25	8	0	—	8
L2a	Pressure	1,190	551	46	15	0	—	6
L2a and L3	Pressure	1,212	281	23	10	1	—	—
L2a and L3	Iontophoresis	807	268	33	6	0	—	—

The cases are ordered by their injection sites. No notable differences in the patterns of labeling were detected between injections restricted to one layer and those involved with two layers.

*The extent of the column was determined by the distribution of labeled neurons. Labeled fibers mostly coursed within the column but also extended beyond its borders. The long and short axes of the column were measured from a single section for each case. Ratio refers to the length of the short axis divided by that of the long axis.

†The numbers of labeled neurons were counted for each layer of each case. Neurons were counted from either one section or two adjacent sections for each case. Labeled neurons in the layer(s) in which the injection site was located were not counted.